International Journal of
Mathematical Modelling & Computations
Vol. 09, No. 02, Spring 2019, 123- 147

Markov Chain Analogue Year Daily Rainfall Model and Pricing of Rainfall Derivatives

T. Berhane[a,*], N. Shibabaw[b] and T. Kebede[c]

[a,b,c] *Department of Mathematics, Bahir Dar University, P.O.Box 79, Bahir Dar, Ethiopia.*

Abstract. In this study we model the daily rainfall occurrence using Markov Chain Analogue Year model (MCAYM) and the intensity or amount of daily rainfall using three different probability distributions; gamma, exponential and mixed exponential distributions. Combining the occurrence and intensity model we obtain Markov Chain Analogue Year gamma model (MCAYGM), Markov Chain Analogue Year exponential model (MCAYEM) and Markov Chain Analogue Year mixed exponential model (MCAYMEM). The models are assessed using twenty nine-years (1987-2015) of historical records of daily rainfall data taken from three different locations which are obtained from Ethiopian National Meteorology Agency (ENMA). Both maximum likelihood and least square techniques are used in the estimation of model parameters. The results indicate that all the three model are suitable for the simulation of precipitation process. In order to assess their performance we apply both qualitative (graphical demonstration) and quantitative techniques. In the quantitative, the performance of the three models; MCAYEM, MCAYGM and MCAYMEM are measured using mean absolute error(MAE) and have mean absolute error of 0.45mm, 0.57 mm and 0.42mm respectively for kiremet(June to September) rainfall which is the long rainy season in Ethiopia. These accuracy is mainly because of the new component that is Analogue Year (AY) used in the modeling of frequency of daily rainfall included in the Markov chain (MC) process. Based on the results of these models we obtain an option price for Teff crop for different months. The result shows an excellent accuracy with only maximum absolute error of 0.54 currency.

Received: 15 February 2019, Revised: 05 April 2019, Accepted: 10 June 2019.

Keywords: Analogue year ; Exponential distribution; Gamma distribution; Markov chain; Option price; Teff.

Index to information contained in this paper

1 **Introduction**
2 **Materials and method**
3 **Result and discussion**
4 **Conclusion**

1. Introduction

Weather derivatives are financial methods used to hedge risks caused by bad weather condition or weather fluctuation . It states how payment will be settled

*Corresponding author. Email: tesfahunb2002@gmail.com

between the parties involved based on the existing weather conditions during the contract period [28]. Commonly weather derivatives are swaps, futures and options based on different weather measures [2]. Unlike traditional derivatives or insurance, Weather derivatives, have no underlying tradable instrument or stock and they cannot be used to hedge price risk because the weather itself cannot be priced, instead, they are used to hedge against other risks for instance agricultural yield risk which are affected by bad weather conditions. Farmers in developing countries are not covered by government sponsored insurance programs but the weather risk is common in large scales. One of the mechanism to protect agricultural output risk is weather derivatives.

Ethiopian economy is highly dependent on the agricultural sector, which accounts around 52% of the gross domestic product (GDP), source of 85% of foreign exchange earnings and job opportunists for about 80% the population in the country [15]. Agriculture in Ethiopia is highly dependent on rainfall, with irrigation agriculture contribute not more than 1% of the country's total cultivated land. As a result, the timely distribution and the amount of rainfall during the growing period are very important or crucial to agricultural output and cause food scarce and famine[11]. Delay on set dates, occurrence in scarce amount and variability of rainfall has great contribution in the reduction of crop yield with significant amount [30]. Rainfall variability usually result in reduction of 20% production and 25% raise in poverty rates in Ethiopia [13, 34]. This rainfall variability has a great impact on the income of every house holds rely on agriculture. In the near future climate conditions are expected to affect the economy of Ethiopia in general and its agriculture sector in particular in reasonable amount and cause 0.5-2.5% decline in GDP per year; for instance rainfall fluctuation alone could contribute a loss of 2 billion USD in the sector [6]. In generally agriculture is the back bone of Ethiopian economy, which is largely dependent on natural rainfall [4, 46]. Therefore, modeling and pricing rainfall derivative is very important for the country in order to reduce these risks. As per the knowledge of the researchers, such kind of work is new (the first) in the described location, as well as in the country Ethiopia. This paper has two main objectives, the first objective is to present a daily rainfall model and the second objective is using the result of the daily rainfall model we calculate an option price for rainfall derivatives. The paper is structured as follows. section 2 materials and methods including major crops and their response to water stress, section 3 result and discussion and section 4 conclusion.

2. Materials and method

Daily rainfall data were collected from Ethiopia National Meteorology Agency (ENMA). In this study we consider twenty nine years of daily rainfall data from three different locations; Debre Markos, Dejen and Gonder, from January 1, 1987-December 31, 2015. The data is classified in to two ; twenty eight years of data is used to model fitting that is for model parameter estimation and the last year of the recorded data is used for model validation purpose that means for comparison. In this paper we use Markov chain analogue year (MCAY) model in order to describe the occurrence or frequency of daily rainfall and three different distributions are used in order to model the amount of rainfall on a wet day. The distributions are exponential distribution, mixed exponential distribution and gamma distribution. The inclusion of the analogue year (AY) component in the frequency modeling part makes these models different from existing models in literature.

The following four points are the basic characteristics of a daily rainfall that should be considered during modeling [32]. First, daily rainfall occurrence probabilities has a seasonal pattern. Second, rainy and dry days have autoregressive property. Third the magnitude of daily rainfall changes with the season and finally the variation in amount of daily rainfall varies with season. In this paper we model the occurrence or nonoccurence of daily rainfall X_t and amount of daily rainfall Y_t separately and combine them to obtain a model for daily rainfall R_t on day t which is given as the product of the occurrence X_t and the amount Y_t as given in (1). Both components of the daily rainfall model are described in detail in the next subsections.

$$R_t = X_t Y_t \tag{1}$$

2.1 *The occurrence process (frequency modeling)*

The existence or nonexistence of daily rainfall X_t is modeled as follow [8, 19, 32]:

$$X_t = \begin{cases} 0, \text{ if day } t \text{ is dry,} \\ 1, \text{ if day } t \text{ is rainy.} \end{cases} \tag{2}$$

where X_t is a two state first order Markov chain with analogue year component so that the probability of rainfall occurrence depends only on the situation from the previous day. The probability of a rainy day followed by a dry day denoted by p_t^{01} and a rainy day followed by a rainy day is represented by p_t^{11}, these probability are known as transition probabilities and given by:

$$p_t^{01} = Pr\{X_t = 1|X_{t-1} = 0\}$$
$$p_t^{11} = Pr\{X_t = 1|X_{t-1} = 1\}$$

Since rainfall occurrence varies with season the transition probabilities are modelled to change daily within a year in order to handle this variation and are approximated by truncated Fourier series.

$$\psi_{ti} = a_{i0} + \Sigma_{k=1}^{m_i} \left[a_{ik} cos\left(\frac{2\pi tk}{365}\right) + b_{ik} sin\left(\frac{2\pi tk}{365}\right)\right] \;\; ; \; i = 1, 2. \tag{3}$$

where $p_t^{01} = \frac{exp(\psi_{t1})}{1+exp(\psi_{t1})}, p_t^{11} = \frac{exp(\psi_{t2})}{1+exp(\psi_{t2})}$ and m_i determines the number of cosine and sine terms required to describe the seasonal cycles. Here we use the logistic function that is $f(x) = \frac{exp(x)}{1+exp(x)}$ for the purpose of transforming the transition probability to the interval (0,1). Based on Akaike information criterion (AIC) and Bayesian information criterion (BIC) we chose $m = 1$ for p_t^{01} and $m = 2$ for p_t^{11}, which give us better result. The coefficients of the Fourier series are estimated by least squares method. In this paper in addition to the transition probability we use the concept of analogue year, that is what was happened on the same date of the previous year. Which improves the accuracy of our model and the concept is not yet used by any other researchers and it is given by (5). In general in this study the occurrence or nonoccurence of rain is modeled using Markov chain analogue year (MCAY). The occurrence process X_t can be generated recursively by using a uniform random variable $u_{1,t} \sim$ *u(0,1)* and a starting value X_0: For $1 \le t \le 365$

$$X_t = \begin{cases} 1, \text{ if } p_t^{x1} \ge u_{1,t}, \\ 0, \text{ otherwise.} \end{cases} \tag{4}$$

And for $366 \leq t \leq n$

$$X_t = \begin{cases} 1, \text{ if } X^h_{(t-365)} \geqslant r_{min} \text{ and } p^{x1}_t \geq u_{1,t}, \\ 0, \text{ otherwise.} \end{cases} \quad (5)$$

where p^{x1}_t as an abbreviation of p^{01}_t and p^{11}_t, X^h_t the historical (observed) rainfall on day t and r_{min} describes the minimal amount that is detected as rain(0.1inch=0.254mm)
Tables 1-6 reveal the parameters of the Fourier series in (3) for Debre Markos, Dejen and Gonder rainfall respectively.

Table 1. Coefficient of ψ_{ti} for p^{01}_t for Debre Markose rainfall.

Coefficient	a_0	a_1	a_2
Value	3.6872	-1.9561	-3.8959

Table 2. Coefficient of ψ_{ti} for p^{11}_t for Debre Markos rainfall.

Coefficient	a_0	a_1	a_2	a_3	a_4
Value	3.6872	-1.9561	1.7091	-3.8959	0.2183

Table 3. Coefficient of ψ_{ti} for p^{01}_t for Dejen rainfall.

Coefficient	a_0	a_1	a_2
Value	3.8161	-1.9027	-4.3161

Table 4. Coefficient of ψ_{ti} for p^{11}_t for Dejen rainfall.

Coefficient	a_0	a_1	a_2	a_3	a_4
Value	3.8161	-1.9027	2.1188	-4.3161	0.6243

Table 5. Coefficient of ψ_{ti} for p^{01}_t for Gonder rainfall.

Coefficient	a_0	a_1	a_2
Value	3.1969	-1.8906	-4.0793

Table 6. Coefficient of ψ_{ti} for p^{11}_t for Gonder rainfall.

Coefficient	a_0	a_1	a_2	a_3	a_4
Value	3.1969	-1.8906	1.5661	-4.0793	1.3059

2.2 *Magnitude modeling*

In order to model the magnitude or amount of the rainfall conditional on the fact that it rains on that particular day is done by fitting a distribution to the data. In order to identify a proper distribution to fit the data, first, the histogram of the daily rainfall is examined. Different distributions with a nonnegative domain have been proposed to fit historical rainfall data in literature. Among these distributions a gamma distribution is proposed by [1, 5, 10, 21, 28, 31, 44, 48, 52] and exponential distribution was used by [37, 47, 49] while a mixed exponential distribution is proposed by [16, 24, 38, 45, 52–54]. Woolhiser and Todorovic in 1975 were the first who proposed the mixed exponential distribution to model rainfall amount [52]. Mixed exponential distribution has the advantage of a better representation to extreme events [52]. Similarly, in [33], a beta distribution is found to provide the better fit in data. In this work we consider three nonnegative distributions, these are gamma distribution, exponential and mixed exponential distribution to model the intensity or amount of daily rainfall.

2.2.1 Gamma distribution

The gamma distribution function is a continuous probability distribution with two parameters α is called the shape parameter and β is called the scale parameter and it is defined by the following probability density function (PDF)

$$f(x) = \begin{cases} \frac{(x/\beta)^{\alpha-1}e^{-x/\beta}}{\beta\Gamma(\alpha)}, & \text{if } x, \alpha, \beta > 0 \ , \\ 0, & \text{otherwise.} \end{cases} \tag{6}$$

Where

$$\Gamma(\alpha) = \int_0^\infty t^{\alpha-1}e^{-t}dt \tag{7}$$

The value of the shape parameter is greater than zero and it determines the level of positive skewness on the other hand the scale parameter β of gamma distribution determines the spread of values, widening when β is large and narrowing when β is small. Due to flexible representation of variety of distribution shapes which involves small number of parameters that is shape and scale parameter only , the gamma distribution commonly used to describe rainfall amount and assumed to be appropriate distribution to represent rainfall amount [36, 39, 43, 49, 50]. The appropriateness of the gamma distribution has been proven by different scholars some of them are given in these references [7, 17, 18, 22, 25, 35, 57]. In Figure 1 we plot five different gamma probability distribution to demonstrate the existence of variety of shapes in the gamma distribution. The mean and variance of gamma distribution are $\alpha\beta$ and $\alpha\beta^2$ respectively.

2.2.2 Exponential distribution

The family of exponential distributions provides probability models that are very widely used in engineering and science disciplines. A random variable X is said to have an exponential distribution with parameter $\mu > 0$ if the probability distribution function(PDF) of X is

$$f(x) = \begin{cases} \frac{1}{\mu}e^{\frac{-x}{\mu}} & \text{for } \mu > 0, x \geq 0 \ , \\ 0, & \text{otherwise .} \end{cases} \tag{8}$$

where the parameter μ is the mean of the exponential distribution distribution. And the cumulative distribution function (CDF) of the exponential distribution is given by

$$F(x) = \begin{cases} 1 - e^{\frac{-x}{\mu}} & \text{for } \mu > 0, x \geq 0 \ , \\ 0, & \text{otherwise .} \end{cases} \tag{9}$$

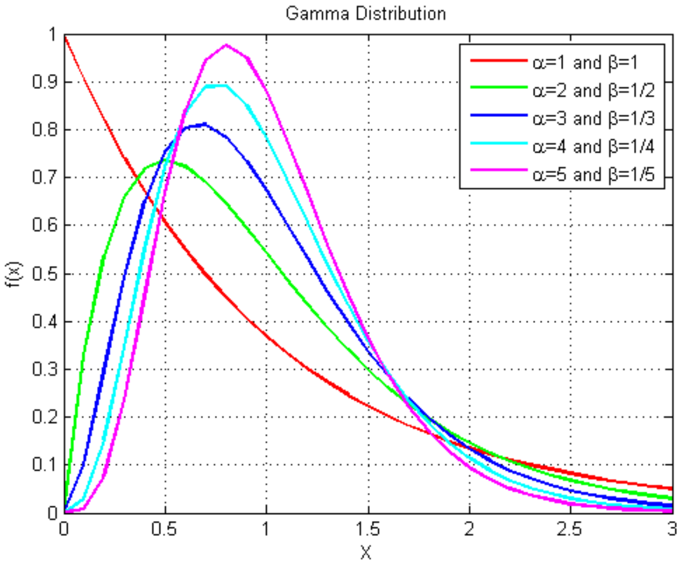

Figure 1. Gammma distribution with different shape and scale parameters.

Figure 2 reveals graph of exponential distribution with different values of μ.

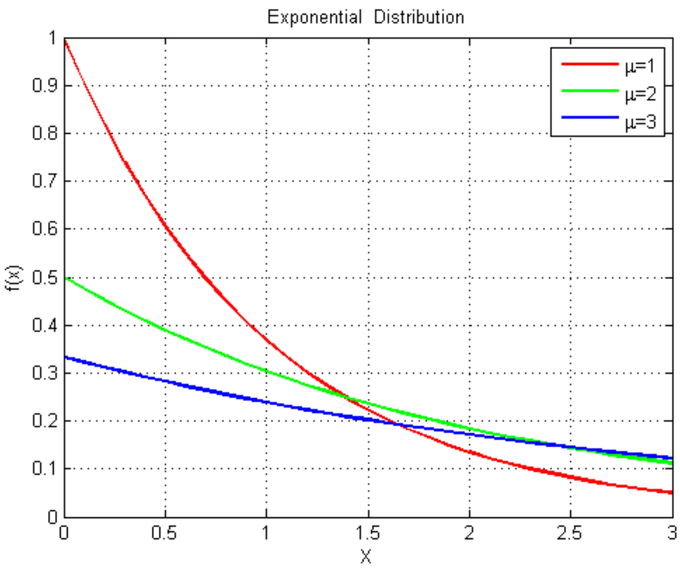

Figure 2. Exponential distribution with different parameters (μ values).

2.2.3 Mixed exponential distribution

The mixed exponential distribution is a weighted combination of two exponential distributions and inherits their properties. The mixed exponential distribution for a random variable X is defined by the following probability density function (PDF):

$$f_{mix}(X) = \frac{\alpha}{\beta_1} e^{\frac{-X}{\beta_1}} + \frac{1-\alpha}{\beta_2} e^{\frac{-X}{\beta_2}} \tag{10}$$

with $0 < \beta_1 \leqslant \beta_2$ and $0 < \alpha < 1$ and the cumulative density function (CDF) is defined by

$$F_{mix}(X) = \alpha e^{\frac{-X}{\beta_1}} + (1-\alpha)e^{\frac{-X}{\beta_2}} \tag{11}$$

where, β_1 and β_2 are the parameters of the two exponential distribution respectively which represents the mean of the distributions and α is the mixing parameter. The contribution of the component probability density functions are determined by the mixing parameter α, that means α tell us with what probability the random variable X sampled from the individual distributions. The mean μ and variance σ^2 of the mixed exponential distribution are given by $\mu = \alpha\beta_1 + (1-\alpha)\beta_2$ and $\sigma^2 = \alpha\beta_1^2 + (1-\alpha)\beta_1^2 + \alpha(1-\alpha)(\beta_1 - \beta_2)^2$ where β_1 and β_2 are the means of the component distributions. Sampling or generating a random variable X from mixed exponential distribution is a two step procedure, first a component distribution is chosen based on the mixing parameter α then a random variable from the selected component distribution is generated and returned as the simulated sample from the mixture. Since rainfall amount varies seasonally, in order to maintain its seasonality, we determine the parameters for each month so that it varies monthly with in a year and remains constant across different years, that is for each month we obtain its own distribution parameters. The parameters α, β_1 and β_2 of the mixed exponential distribution are estimated using maximum likelihood estimators and the daily rainfall amount process simulated with two independent uniform random variables $u_{2,t}, u_{3,t} \sim u(0,1)$, independent from $u_{1,t} \sim u(0,1)$ using standard inverse transform sampling method given in (12) [8, 28, 29].

$$Y_t = -\phi_t ln(u_{2,t}), \tag{12}$$

where Y_t represents the amount of rainfall on day t and ϕ_t is given by

$$\phi_t = \begin{cases} \beta_{1,t}, & \text{if } \alpha_{t,k} \geq u_{3,t} \ , \\ \beta_{2,t}, & \text{if } \alpha_{t,k} < u_{3,t} \ . \end{cases} \tag{13}$$

After the estimation of the occurrence and the amount processes, they can be combined to simulate rainfall using (1). Using this daily simulation rain fall index is obtained. Rainfall index $I(\tau_1, \tau_2)$ over the period (τ_1, τ_2) is defined as the sum of the daily rainfall R_t for a particular location with accumulation period (τ_1, τ_2), which is known as cumulative rainfall (CR) it is given by (14).

$$CR = \sum_{\tau_1}^{\tau_2} R_t \tag{14}$$

2.2.4 Fitting distributions to daily rainfall

2.3 *Parameter estimation*

The maximum likelihood estimation method (MLE) is used for parameter estimation because this approach performs much better than other methods [51]. The MLE method determines a set of parameters which maximize the likelihood function (as the name suggests, the method seeks to find values of the distribution parameters that maximize the likelihood function). The parameters are obtained by differentiating the log likelihood function with respect to the parameters of the

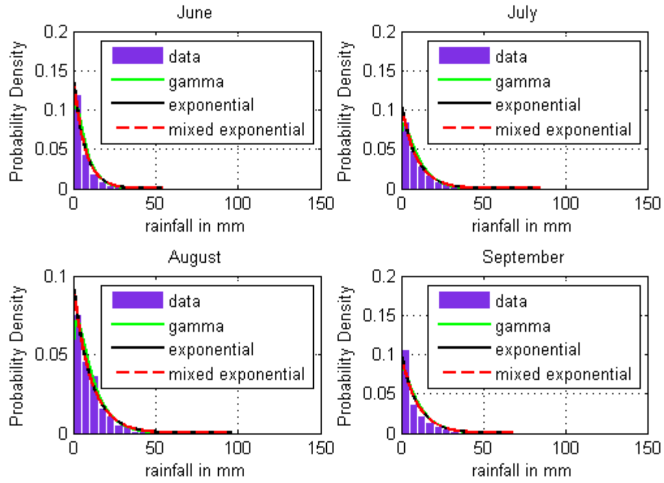

Figure 3. Comparison of the histogram of June-Septemper wet days with Exponential, Gamma and mixed exponential probability density functions for Debremarkos, Ethiopia.

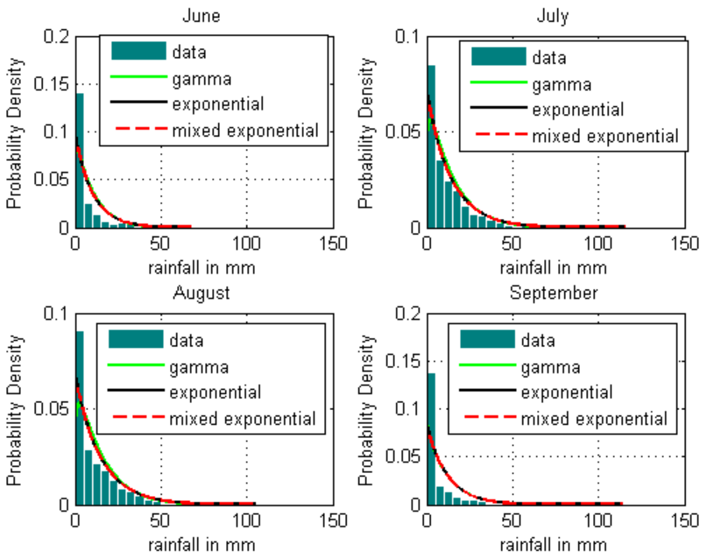

Figure 4. Histogram for June-September wet days and fitted exponential, gamma and mixed exponential probability density function for Dejen, Ethiopia.

distribution. The likelihood function for the gamma distribution is:

$$L(x;\alpha,\beta)=\prod_{i=1}^{N} f(x_i;\alpha,\beta) \tag{15}$$

Since maximizing the log equivalent to maximizing the likelihood function and working on addition is simpler than on working on multiplication we use the log-likelihood function and it is defined as:

$$lnL=\sum_{i=1}^{N}\frac{(x_i/\beta)^{\alpha-1}e^{-x_i/\beta}}{\beta\Gamma(\alpha)}=-Nln\Gamma(\alpha)-N\alpha ln\beta+(\alpha-1)\sum lnx_i-\sum\frac{x_i}{\beta} \tag{16}$$

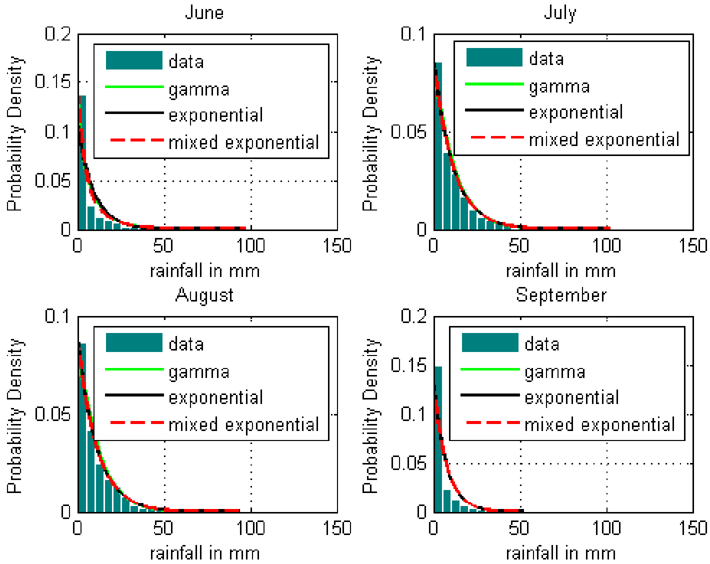

Figure 5. Comparison of the histogram of June-Septemper wet days with Exponential, Gamma and mixed exponential probability density functions for Gonder, Ethiopia.

In the following we describe maximum likelihood estimator for mixed exponential distribution. Probability density function (PDF) of the mixed exponential distribution is given in (17).

$$f(x;\alpha,\beta_1,\beta_2) = \frac{\alpha}{\beta_1}e^{\frac{-x}{\beta_1}} + \frac{1-\alpha}{\beta_2}e^{\frac{-x}{\beta_2}} \tag{17}$$

Define the log-likelihood function

$$\begin{aligned} l(x;\alpha,\beta_1,\beta_2) &= \sum_{i=1}^{N} ln(f(x_i;\alpha,\beta_1,\beta_2)) \\ &= \sum_{i=1}^{N} ln\left(\frac{\alpha}{\beta_1}e^{(\frac{-x_i}{\beta_1})} + \frac{1-\alpha}{\beta_2}e^{(\frac{-x_i}{\beta_2})}\right) \\ &= \sum_{i=1}^{N} ln\left(\frac{\alpha}{\beta_1}\right) - \sum_{i=1}^{N}\frac{x_i}{\beta_1} + \sum_{i=1}^{N} ln\left(\frac{1-\alpha}{\beta_2}\right) - \sum_{i=1}^{N}\frac{x_i}{\beta_2} \\ &= Nln\left(\frac{\alpha}{\beta_1}\right) - \sum_{i=1}^{N}\frac{x_i}{\beta_1} + Nln\left(\frac{1-\alpha}{\beta_2}\right) - \sum_{i=1}^{N}\frac{x_i}{\beta_2} \end{aligned} \tag{18}$$

Set the derivative of (18) equal to zero to find the maximum.

$$\frac{\partial l(x_i;\alpha,\beta_1,\beta_2)}{\partial \alpha} = 0 \tag{19}$$

$$\frac{\partial l(x_i;\alpha,\beta_1,\beta_2)}{\partial \beta_1} = 0 \tag{20}$$

$$\frac{\partial l(x_i;\alpha,\beta_1,\beta_2)}{\partial \beta_2} = 0 \tag{21}$$

The derivative give us the following equations

$$\frac{N}{\alpha} - \frac{N}{1-\alpha} = 0 \tag{22}$$

$$\frac{-N}{\beta_1} + \sum_{i=1}^{N} \frac{x_i}{\beta_1^2} = 0 \tag{23}$$

$$\frac{-N}{\beta_2} + \sum_{i=1}^{N} \frac{x_i}{\beta_2^2} = 0 \tag{24}$$

Similarly the likelihood of the exponential distribution is obtained as follow:

$$f(x;\mu) = \frac{1}{\mu} e^{\frac{-x}{\mu}} \tag{25}$$

Define the log-likelihood function

$$\begin{aligned} l(x;\mu) &= \sum_{i=1}^{N} ln(f(x_i;\beta)) \\ &= \sum_{i=1}^{N} ln\left(\frac{1}{\mu} e^{\frac{-x_i}{\mu}}\right) \\ &= \sum_{i=1}^{N} ln\left(\frac{1}{\mu}\right) - \sum_{i=1}^{N} \frac{x_i}{\mu} \\ &= Nln\left(\frac{1}{\mu}\right) - \sum_{i=1}^{N} \frac{x_i}{\mu} \qquad (26) \\ &= -Nln\mu - \sum_{i=1}^{N} \frac{x_i}{\mu} \qquad (27) \end{aligned}$$

2.4 *Major crops and their response to water stress*

Major crops in Ethiopia in terms of area of land coverage and contribution to the country's production are Teff, Maize, Sorghum, Wheat and Barely. They are produced using rainfall as source of water supply. Defining the crop water requirement during its various stages of growth and development in terms of potential evapo-transpiration and comparing these requirements with the water available at the time can obtain the effect of rainfall on the crops. When water supply that is rainfall does not meet crop water requirement, crops vary in their response to water deficient. In some crops there is an increase in water utilization efficiency (amount of harvested yield produced by the crop per unit of water evapo-transpired) whereas for other crops it decreases with increase in water deficient [12]. When water deficiency occurs during a particular part of the total growing period of a crop, the yield response to water deficient can vary greatly depending on how sensitive the crop is at that growing period. In general, crops are more sensitive to water deficient during emergence, flowering and early yield formation than they are during early (vegetative, after establishment) and late growing periods (ripening) [12]. However, the response of yield to water cannot be considered in isolation from all other agronomic factors, such as fertilizers, plant density and crop protection, because these factors also determine the extent to which actual yield approaches maximum yield [12]. In the following subsections, we tried to discuss some major crops growing period, water requirement and water stress condition in Ethiopia based on documents of Ethiopian Agricultural Research Organization (EARO) and FAO Irrigation and Drainage papers[12].

2.4.1 Teff

Teff is one of the major cereal crops originated and diversified in Ethiopia and it is the most common cereal crops cultivated in the country and it covers around 29% of the area of land used for cultivation of cereal crops [20, 26]. The average yield of Teff per hectare is about 1.56 tons and it accounts 20% of the total cereal production in the country [9]. Teff contains about 11% protin with an excellent source of important amino acids like lysine which is the amino acid mostly scarce in other grains. The other important feature of teff is the glycemic index is low, so that people with Type 2 diabetes make it first choice of their diet and teff also contains minerals such as iron, potassium, calcium and phosphorus . In addition to these teff is consumed by gluten intolerant people since teff contains gluten lacking the gladian fraction that causes coeliac disease [27]. Teff can be stored for several years with out being damaged by insects. Due to these and other reasons currently teff is cultivated outside its origin such as the United States, Netherlands, Canada, Australia, China, India, the UK, Cameroon, South Africa, Uganda and Kenya [42]. Areas with altitude 1700m to 2400m and average annual rainfall 1000 mm during the growing season is suitable for better production. Even though the time of sowing varies according to the type of soil and the appearance of the big rains, for better productivity, sowing can take place from the second week of July to the third week of July for light soil and it is more advisable to sow later generally during the last two weeks of the month of July [40]. Crop coefficient K_c is the ratio of crop evapotranspiration (ET_c) to reference crop evapotranspiration (ETo) that can be established based on crop evapotranspiration and climate [3, 55]. It is a function of climate, crop type, crop growth stages, soil moisture and irrigation method[23, 41]. The crop coefficient relating water requirement to reference evapotranspiration during its growing period in Abbay basin is given in Table 7 [40]:

Table 7. Crop coefficient of Teff.

Month	June	July	August	September
K_c	0.3	0.7	1.1	0.7

2.4.2 Maize

Maize originated in Central America, where it is traditionally planted in hills. It is an introduced crop to Ethiopia and it has been expanding widely in the recent years because of the very favorable conditions found in large areas of the country. Successfully, it can be grown in a wide range of altitude ranging from lowland areas below 1000m up to 1800m above sea level. And it can be grown preferably in areas where the annual rainfall reaches an average of 800 mm equally distributed over the whole growing period. A major conclusion of research findings from many experiments in EARO [12] concluded on maize during a number of years in Ethiopia is that yield is generally influenced more by the date of sowing than any other factor. Sowing should take place the first two weeks of May or as early as possible at the onset of the big rains. In addition, the growth period is 4 to

5 months even if it depends on the variety planted. The crop factor (K_c) relating water requirement to reference evapo-transpiration (ETo) in Abbay Basin during their growing period is given in Table 8 [40]: Growing stages of maize according to

Table 8. Crop coefficient Maize.

Month	May	June	July	August	September	October
K_c	0.4	0.65	0.85	1.1	0.8	0.3

FAO are classified as establishment (15-25 days), vegetative (25-40 days), flowering (15-20 days), yield formation (35-45 days) and ripening (10-15) [16]. Maize appears relatively tolerant to water shortage during the vegetative and ripening periods. Greatest decrease in grain yields is caused by water deficient during the flowering period. Water deficient during the yield formation period may also lead to reduced yield due to a reduction in grain size. However, water deficient during ripening period has little effect on grain yield.

2.4.3 Wheat

Wheat is a common crop in the highland of Ethiopia. It is highly sensitive to drought and it is not recommended in dry areas. The most suitable areas for wheat production are those with an average annual rainfall of 1200 mm with 600 mm well distributed during the growth period. The crop coefficient (K_c) relating water requirement to reference evapo-transpiration in Abbay basin is given in Table 9 [40]: For better yield, sowing time is the end of June or the early days of July.

Table 9. Crop coefficient of wheat

Month	June	July	August	September	October
K_c	0.8	1.1	1.1	1.05	0.25

And the growing period for different verities are 115-135 days. Growing stages of Wheat according to FAO are classified as establishment (10-15 days), vegetative (10-30 days), flowering (15-20 days), yield formation (30-35 days) and ripening (10-15 days) [12]. Slight water deficient in the vegetative period may have little effect on crop development or may even somewhat hasten maturation. The flowering period is most sensitive to water deficient. Water deficient during the yield formation period results in reduced grain weight and, during the ripening period has a slight effect on yield. Tables 10, 11 and 12 show the correlation between monthly average rainfalls and cereal production in Amhara National Regional State [4].

Table 10. Correlations between production of Teff and monthly rainfalls in the ANRS.

Month	June	July	August	September
correlation	0.189	0.199	0.623	0.493

Table 11. Correlations between production of maize and monthly rainfalls in the ANRS.

Month	May	June	July	August	September
correlation	0.309	0.188	0.345	0.349	0.149

Table 12. Correlations between production of wheat and monthly rainfalls in the ANRS.

Month	June	July	August	September
correlation	0.414	0.612	0.564	0.733

2.5 *Valuation of rainfall options*

In this paper to obtain an option price for rainfall we follow the approach used in [33]. To calculate a weather derivative contract we consider the following important points [56]: Type of contract, time of contract (length of the contract period), meteorological weather station from which the data is taken, the weather index (I) for the weather derivative, strike level (S) or pre-negotiated threshold for the weather index I, the amount of money k per unit index which is known as tick size (k) or constant payment (P_o) per unit index and the amount of money that you pay for an insurance when you buy it known as premium. Call and put options are the main types of options used in the weather risk-management market. A call contract involves a buyer and a seller who first agree on a contract period and a weather index (I_t) that serves as the basis of the contract. At the start of the contract, the seller receives a premium from the buyer. In return, during the contract or at the end of the contract period, if I_t is greater than the pre-negotiated threshold or strike (S), the seller pays the buyer an amount given by equation (28) [32].

$$P_{call} = k * max(I_t - S, 0) \tag{28}$$

where: k (tick) is a pre-agreed upon constant factor that determines the amount of payment per unit of weather index. A fixed amount P_o is paid if I_t is greater than S, or no payment is made otherwise. A put option is the same as a call option except that the seller pays the buyer when I_t is less than S [33].

$$P_{put} = k * max(S - I_t, 0) \tag{29}$$

A call and a put are basically equivalent to an insurance policy: the buyer pays a premium, and in return, receives a commitment of compensation when a predefined condition is met [14]. The price of an option (or its premium) is calculated from the expected payoff as [2]:

$$c = exp(-r(\tau_2 - t))P \tag{30}$$

where c is the premium that the hedgers (buyers) need to pay for a contract, r is a risk-free periodic market interest rate, t is the date that the contract is issued (purchased), and τ_2 is the date the contract is claimed or the expiration date. P is the payoffs based on the predicted rainfall. Table 13 reveals the option specifications for pricing of rainfall derivatives which is the approach used by Oliver Musshoff Martin *et al.* [33].

3. Result and discussion

In this section, we present results in terms of figures, tables and a discussion of them. Tables 14, 15 and 16 reveal the maximum likelihood estimates of the exponential, mixed exponential and gamma distribution parameters for each of the 12 months in the three locations under study. All the parameters are determined with 95% confidence level. In Figure 9a and 9b we present the comparison of the occur-

Table 13. Specifying options.

Type	Put option	Call option
Payoff	$k * max(S - I_t, 0)$	$k * max(I_t - S, 0)$
Strike S	S	S
Index I_t	$\Sigma_{t=\tau_1}^{\tau_2} R_t$	$\Sigma_{t=\tau_1}^{\tau_2} R_t$
Tick value k	1 currency	1 currency
Maturation date	1 month	1month

Table 14. Estimated parameter for Debre Markos station.

	Exponential	Gamma		Mixed Exponential		
Month	μ	α	β	α	β_1	β_2
January	4.4378	0.8746	5.0308	0.6981	2.3387	9.2892
February	4.4561	1.0363	4.2979	0.2584	1.6383	5.4376
March	5.7492	0.9904	5.7662	0.5580	3.4180	8.6938
April	6.4531	0.9322	6.7946	0.4108	3.0380	8.8503
May	7.2653	0.9832	7.6101	0.1872	3.1091	8.2228
June	7.1096	1.2121	5.8087	0.0100	4.4417	7.1365
July	9.4395	1.2184	7.6475	0.0100	6.4556	9.4667
August	10.8063	1.2481	8.5413	0.0158	10.6913	10.8080
September	10.0271	1.1205	8.8624	0.0100	5.0139	10.0738
October	9.2975	1.0122	9.0119	0.9320	2.2056	9.8152
November	5.8059	0.9174	6.4382	0.4379	2.5491	8.3434
December	6.1988	0.9706	6.2147	0.6169	3.8966	9.9052

Table 15. Estimated parameter for Dejen station.

	Exponential	Gamma		Mixed Exponential		
Month	μ	α	β	α	β_1	β_2
January	4.9894	0.7421	6.7230	0.4391	1.6064	9.3116
February	5.1366	0.9147	5.6158	0.6793	2.5676	10.5790
March	8.9327	0.9461	9.4415	0.1951	2.7966	10.4200
April	7.3373	1.0061	7.2930	0.3914	11.9300	4.3821
May	9.2221	0.9849	9.3631	0.3083	4.4023	11.3690
June	10.3270	1.0803	9.5592	0.0193	4.3882	10.4490
July	13.9760	1.1676	11.9700	0.0010	6.6530	13.9760
August	14.5780	1.1960	12.1890	0.0018	1.5363	14.5840
September	11.9000	0.9813	12.1280	0.0100	0.8873	11.900
October	12.9520	0.9821	13.1880	0.1110	4.0851	14.0590
November	10.9880	0.8646	12.7080	0.1022	1.3836	12.0810
December	4.3653	0.9062	4.8174	0.2434	1.1398	5.4030

rence of daily rainfall with out the analogue year component that is using only the first order Markov chain (MC) and with the analogue year component that is using the new model Markov chain analogue year model (MCAY). Figure 9a shows the result using MC and Figure 9b presents the occurrence using (MCAY). As clearly observed from the figures, Figure 9b gives a better fit to observed frequency as the plots over lap. Hence, using the analogue year (AY) component in the modeling of the occurrence or non nonoccurence of daily rainfall has a positive significant effect and it is appropriate. Tables from 17-25 shows the comparison of the statistics in all the three models over the three locations. As observed from these tables the

Table 16. Estimated parameter for Gonder station.

	Exponential	Gamma		Mixed Exponential		
Month	μ	α	β	α	β_1	β_2
January	4.4696	0.9929	4.5015	0.4406	1.5085	6.8016
February	4.6370	1.1923	3.8890	0.0100	4.6047	4.6372
March	4.9585	0.8881	5.5831	0.8012	2.7211	13.9751
April	5.3370	0.9245	5.7726	0.8294	4.0414	11.6388
May	7.4058	0.9186	8.0620	0.5371	3.6963	11.7091
June	9.2407	0.8794	10.5078	0.3986	3.8033	12.8483
July	11.4244	1.0807	10.5713	0.0100	2.9121	11.5103
August	11.2280	1.1257	9.9738	0.0100	4.3622	11.2914
September	7.4677	1.0057	7.4253	0.1945	3.1601	8.5078
October	8.2613	0.7090	11.6517	0.4714	2.2984	13.5773
November	5.7755	0.8660	6.6690	0.4855	2.4330	8.9301
December	5.7739	0.8130	7.1021	0.7492	3.3574	12.9879

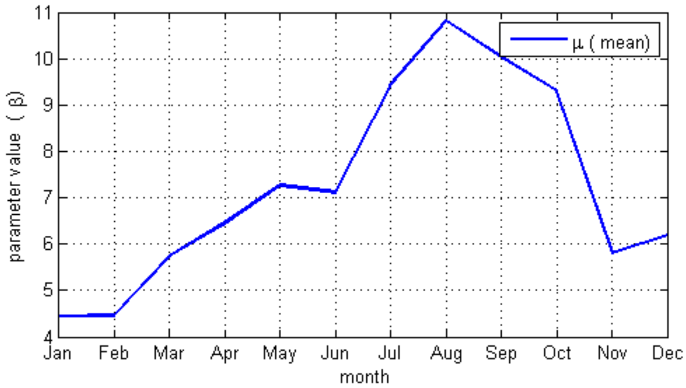

Figure 6. Plot of exponential parameter μ for Debre Markos rainfall.

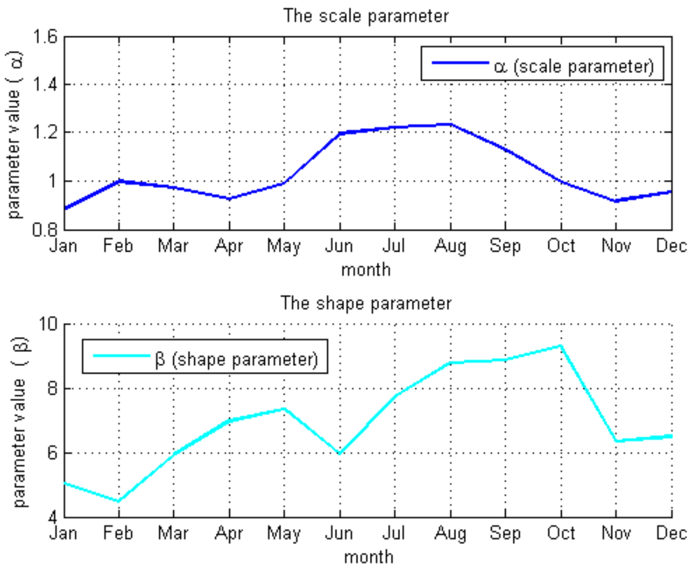

Figure 7. Plot of gamma distribution parameters α and β, Debre Markos rainfall.

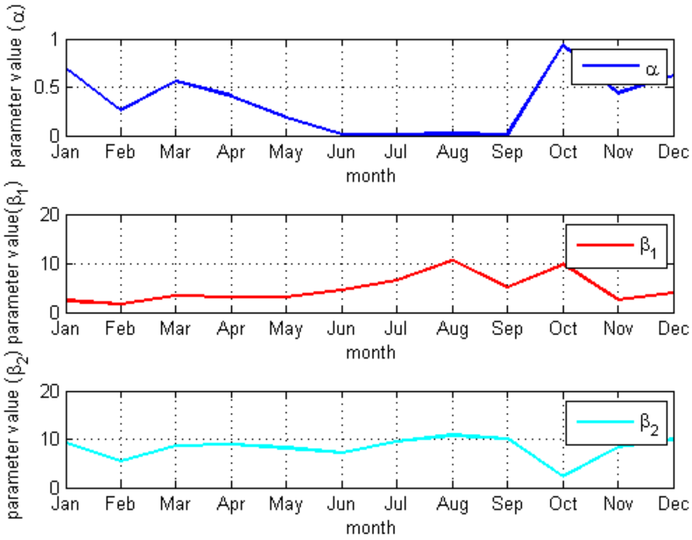

Figure 8. Plot of mixed exponential parameter for each month, Debre Markos rainfall.

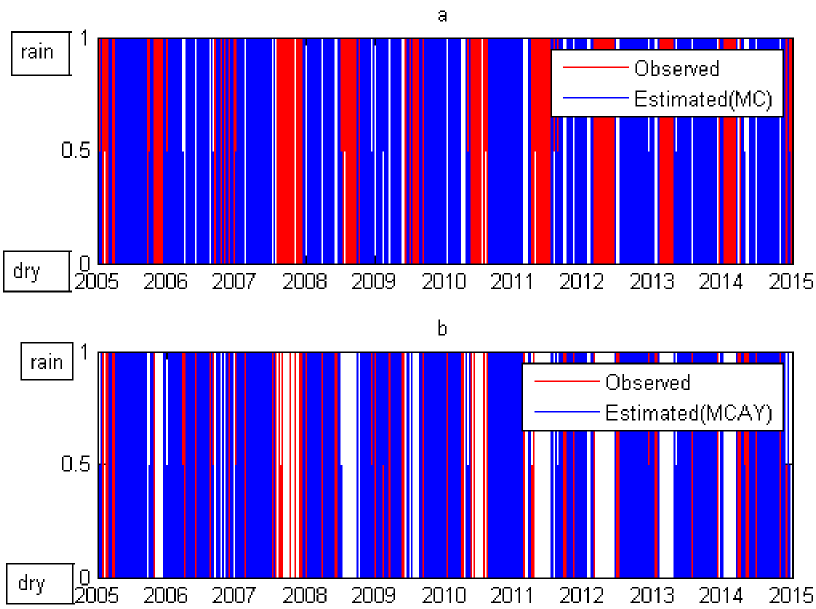

Figure 9. (a) Frequency of rainfall occurrence using MC (Markov chain with out analogue year component) (b) Frequency of rainfall occurrnce using Markov chain with the analogue year component (MCAY) model.

absolute error in the approximation of the mean for instance using MCEM, MCGM and MCMEM (without the AY component) ranges from minimum 2.8294 to maximum 5.2657 where as in the case of MCAYEM, MCAYGM and MCAYMEM (with the AY component) the absolute error in the approximation of the mean ranges from minimum 0.0099 to maximum 0.1618. Therefore it is one evidence for the goodness of the models as well as the nobility of the AY component incorporating in the Markov chin to model the occurrence of daily rainfall. Table 26 presents the summary of the absolute errors in the approximation of basic statistics using existing models (without the analogue year component) and the new models (with the analogue year component). Table 26 presents the summary of the absolute

Table 17. Comparison of the statistic of observed with MCEM (existing model) and MCAYEM(new model) for Dejen raifall.

Statistics	observed	MCEM	AE	MCAYEM	AE
Mean	3.7851	9.0508	5.2657	3.7752	0.0099
Standard deviation	8.8384	10.9750	2.1366	8.9431	0.1047
Skewness	3.5920	2.3928	1.1992	3.6628	0.0708
Kurtosis	20.5050	11.5580	8.9470	20.70	0.1950

Table 18. Comparison of the statistic of observed with MCGM (existing model) and MCAYGM (new model) for Dejen raifall.

Statistics	observed	MCGM	AE	MCAYGM	AE
Mean	3.7851	8.8728	5.0877	3.7552	0.0299
Standard deviation	8.8384	10.6830	1.8446	8.8155	0.0229
Skewness	3.5920	2.3208	1.2712	3.7057	0.1137
Kurtosis	20.5050	10.9530	9.5520	21.9680	1.463

Table 19. Comparison of the statistic of observed with MCMEM (existing model) and MCAYMEM(new model) for Dejen raifall.

Statistics	observed	MCMEM	AE	MCAYMEM	AE
Mean	3.7851	8.3976	4.6125	3.6668	0.1183
Standard deviation	8.8384	11.1400	2.3016	8.8155	0.0553
Skewness	3.5920	2.3560	1.2360	3.6497	0.0577
Kurtosis	20.5050	10.6110	9.8940	20.301	0.2040

Table 20. Comparison of the statistic of observed with MCMEM (existing model) and MCAYMEM (new model) for Debre Markos raifall.

Statistics	observed	MCEM	AE	MCAYEM	AE
Mean	3.6573	6.5236	2.8663	3.4879	0.1694
Standard deviation	7.0854	7.9118	0.8264	7.0771	0.0083
Skewness	3.1950	2.6863	0.5087	3.4360	0.5087
Kurtosis	18.0600	15.4170	2.6430	20.1560	2.0960

Table 21. Comparison of the statistic of observed with MCGM (existing model) and MCAYGM (new model) for Debre Markos raifall.

Statistics	observed	MCGM	AE	MCAYGM	AE
Mean	3.6573	6.4867	2.8294	3.4955	0.1618
Standard deviation	7.0854	7.5721	0.4867	6.7750	0.3104
Skewness	3.1950	2.4231	0.7719	3.1853	0.0097
Kurtosis	18.0600	12.9910	5.0690	18.1840	0.124

errors in the approximation of basic statistics using existing model (without the analogue year component) and the new model (with the analogue year component)

On the basis of the developed daily rainfall model, we obtain cumulative monthly rainfall for each month of 2015. Tables 27, 28 and 29 reveal the estimated and observed monthly cumulative rainfall along with the corresponding absolute error (AE). Figure 13 shows the cumulative monthly rainfall of each station and the graphs given in figure 14 presents the mean monthly rainfall of each station. In order to obtain the strike rainfall for each month of the growing period of each crop

Table 22. Comparison of the statistic of observed with MCMEM (existing model) and MCAYMEM (new model) for Debre Markos raifall.

Statistics	observed	MCMEM	AE	MCAYMEM	AE
Mean	3.6573	6.6304	2.9731	3.5957	0.0.0616
Standard deviation	7.0854	8.3334	1.2480	7.3475	0.2621
Skewness	3.1950	2.5593	0.6357	3.4895	0.2945
Kurtosis	18.0600	13.5720	4.4880	20.1160	2.0560

Table 23. Comparison of the statistic of observed with MCEM (existing model) and MCAYEM (new model) for Gonder raifall.

Statistics	observed	MCEM	AE	MCAYEM	AE
Mean	3.1838	6.3711	3.1873	3.1005	0.0833
Standard deviation	7.4994	8.2795	1.7801	7.3018	0.1976
Skewness	3.8193	2.8226	0.9967	3.9575	0.1382
Kurtosis	22.8990	16.0150	6.8440	24.4920	1.5930

Table 24. Comparison of the statistic of observed with MCMEM (existing model) and MCAYMEM (new model) for Gonder raifall.

Statistics	observed	MCMEM	AE	MCAYEM	AE
Mean	3.1838	6.3604	3.1766	3.1251	0.0587
Standard deviation	7.4994	9.0700	1.5706	7.4325	0.0669
Skewness	3.8193	2.8693	0.9500	3.7535	0.0630
Kurtosis	22.8990	14.9750	7.9240	21.7040	1.1950

Table 25. Comparison of the statistic of observed with MCGM (existing model) and MCAYGM (new model) for Gonder raifall.

Statistics	observed	MCGM	AE	MCAYGM	AE
Mean	3.1838	6.6380	3.4542	3.1993	0.0155
Standard deviation	7.4994	8.3058	0.8064	7.3067	0.1927
Skewness	3.8193	2.7578	1.0615	3.7563	0.0630
Kurtosis	22.8990	15.9450	6.9540	23.2830	0.3840

Table 26. Absolute error in the approximation of basic statistics.

	Existing model		New model	
Statistics	minimum	maximum	minimum	maximum
Mean	2.8294	5.2657	0.0099	0.1618
Standard deviation	0.4867	2.3016	0.0083	0.3104
Skewness	0.5087	1.2712	0.0097	0.5087
Kurtosis	2.6430	9.8940	0.1240	2.0960

type first we find the total crop water transpiration coefficient K_c and we calculate the ratio or percentage of the water requirement in each month for a particular crop type. For example for Teff crop in the growing season June to September the

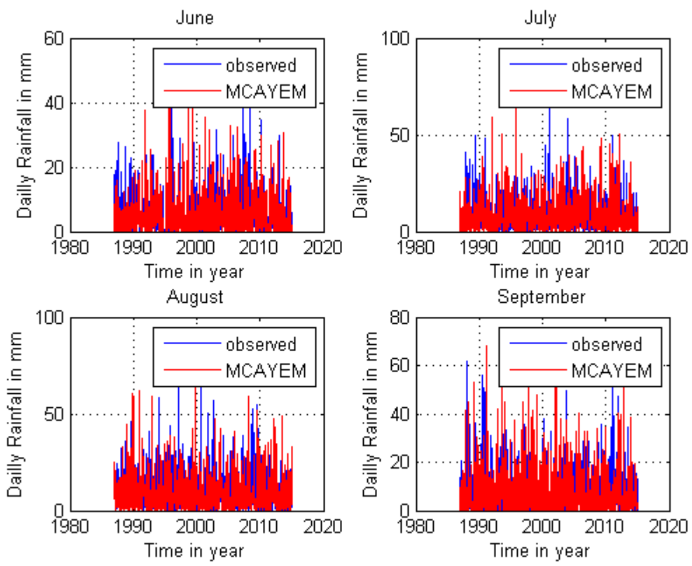

Figure 10. Actual vs estimated daily rainfall of Debre Markos from 1987 to 2015 for months June, July, August and September.

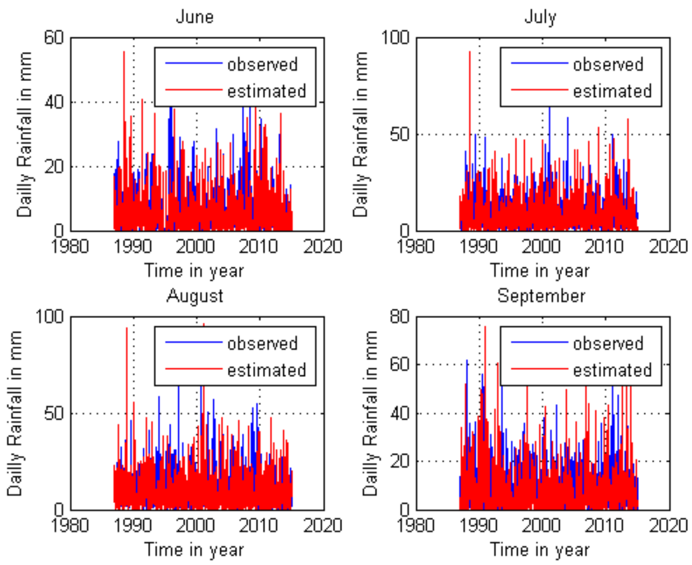

Figure 11. Actual vs estimated daily rainfall of Debre Markose from 1987 to 2015, June-September mixed exponential.

total K_c that is:

$$\sum K_{c_i} = 0.3 + 0.7 + 1.1 + 0.7 = 2.8. \tag{31}$$

Hence the percentage of rainfall required in month i is calculated as:

$$Percentage = \frac{K_{ci}}{\sum K_{ci}} \times 100\% \tag{32}$$

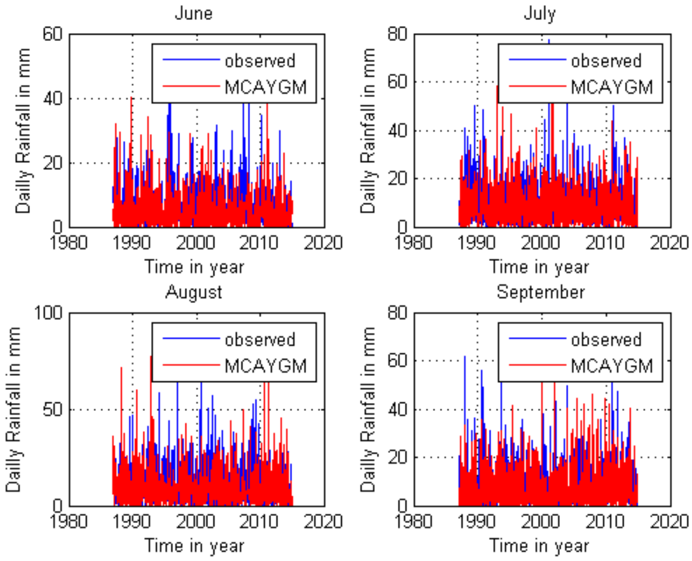

Figure 12. Actual vs estimated daily rainfall of Debre Markose from 1987 to 2015, June-September gamma model.

Table 27. Estimated cumulative monthly rainfall using MCAYMEM, MCAYGM, MCAYEM and the observed monthly cumulative rainfall together with corresponding absolute error (AE) in 2015 of Debre Markos station.

Months	Actual	MCAYMEM	AE	MCAYGM	AE	MCAYEM	AE
January	0.00	0.00	0.00	0.00	0.00	0.00	0.00
February	41.80	32.86	8.94	36.99	4.82	37.03	4.77
March	65.40	65.94	0.54	64.73	0.67	65.85	0.45
April	77.50	78.34	0.84	77.10	0.40	77.48	0.02
May	344.90	344.31	0.59	343.56	1.34	344.22	0.68
June	107.90	108.90	0.56	107.35	0.55	107.38	0.52
July	285.60	285.26	0.34	284.72	0.88	286.27	0.66
August	246.60	246.78	0.18	246.60	0.00	245.83	0.77
September	193.20	193.24	0.04	192.47	0.73	193.04	0.16
October	60.50	60.76	0.26	61.16	0.66	60.52	0.02
November	7.40	0.00	7.40	0.00	7.40	0.00	7.40
December	0.00	0.00	0.00	0.00	0.00	0.00	0.00

For example for June

$$Percentage = \frac{0.3}{2.8} \times 100\% = 10.71\% \tag{33}$$

This means from the total amount of rainfall required for the growth of Teff 10.71% of rainfall expected to fall in the month of June. Moreover, the strike rainfall in each month is obtained by multiplying the total rainfall amount required during the growing season by the corresponding percentage of each month. Table 30 presents the crop coefficient of Teff, the corresponding percentage and amount of rainfall required in each month. Strikes can also obtained by taking the mean of the historical data of each month [14, 38]. For simplicity we take the tick size to be one currency per unit index. Based on the option specification given in Table 13, the option prices are given in Table 31. In this paper we use European option and the trading date for each month is the last date of the immediate previous month.

Table 28. Estimated cumulative monthly rainfall using MCAYMEM, MCAYGM, MCAYEM and the observed monthly cumulative rainfall together with corresponding absolute error (AE) in 2015 of Dejen station.

Months	Actual	MCAYMEM	AE	MCAYGM	AE	MCAYEM	AE
January	0.00	0.00	0.00	0.00	0.00	0.00	0.00
February	34.20	34.54	0.34	33.47	0.73	33.43	0.77
March	10.40	10.79	0.39	11.32	0.92	10.54	0.14
April	0.00	9.17	9.17	9.53	9.53	8.20	8.20
May	185.20	184.81	0.39	185.31	0.12	186.01	0.81
June	89.90	90.78	0.88	89.44	0.46	90.55	0.65
July	129.60	129.10	0.50	129.71	0.11	129.96	0.36
August	333.40	334.35	0.95	333.66	0.26	333.70	0.30
September	166.70	166.95	0.45	167.56	0.86	166.40	0.26
October	29.90	29.09	0.81	30.08	0.18	29.64	0.26
November	110.40	110.65	0.25	110.34	0.06	108.66	1.74
December	5.00	0.00	5.00	0.00	5.00	0.00	5.00

Table 29. Estimated cumulative monthly rainfall using MCAYMEM, MCAYGM, MCAYEM and the observed monthly cumulative rainfall together with corresponding absolute error (AE) in 2015 of Gonder station.

Months	Actual	MCAYMEM	AE	MCAYGM	AE	MCAYEM	AE
January	0.00	0.85	0.85	0.00	0.00	0.39	0.39
February	8.10	0.00	8.10	33.47	0.73	33.43	0.77
March	20.70	20.49	0.21	20.63	0.07	20.74	0.04
April	2.50	10.42	7.92	9.42	6.92	7.45	4.95
May	130.40	130.82	0.42	130.12	0.28	130.86	0.46
June	121.60	121.44	0.16	121.22	0.38	122.07	0.47
July	236.20	236.81	0.61	236.96	0.76	235.76	0.44
August	247.30	247.02	0.28	246.36	0.94	247.43	0.13
September	123.20	123.15	0.05	122.32	0.88	123.90	0.70
October	25.40	24.97	0.43	24.91	0.49	25.48	0.08
November	35.91	34.22	1.69	35.56	0.35	35.74	0.17
December	8.00	0.00	8.00	0.00	8.00	0.00	8.00

Table 30. Crop coefficient of Teff, the corresponding percentage and amount of rainfall required in each month.

Month	June	July	August	September
K_c	0.30	0.70	1.10	0.70
Percentage(%)	10.71	25	39.28	25
Rainfall in mm	107.14	250	392.86	250

For instance for June the trading date is May 30. The result reveals an excellent accuracy with mean absolute error of 0.54 (MCAYMEM), 0.36 (MCAYGM) and 0.34 (MCAYEM). In the same manner one can do for maize and wheat.

4. Conclusion

In this study we model daily rainfall and set an option price for Teff crop for different months in its growing season. The modeling procedure is separated in two parts. The first part is modeling of the occurrence or frequency of rainfall

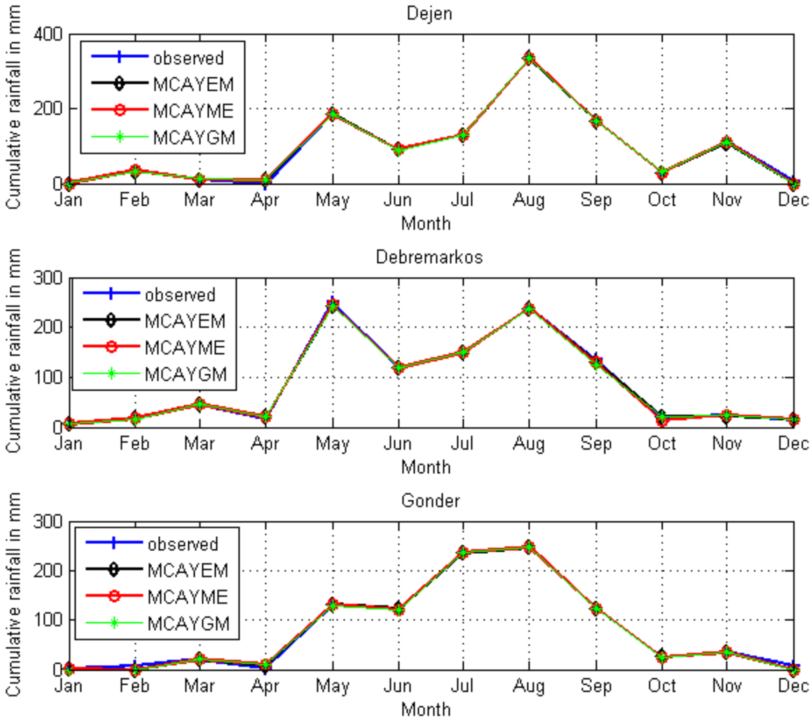

Figure 13. Cumulative montly rainfall using (a) MCAYMEM, (b) MCAYMEM, (c) MCAYMEM (top to bottom) respectively and observed monthly cumulative rainfall of Dejen, Debre Markos and Gonder in the year 2015.

Table 31. Put Option prices with $r = 0.0058$ using MCAYMEM, MCAYGM, MCAYEM and the observed monthly cumulative rainfall together with corresponding absolute error in 2015 of Dejen station.

Months	observed	MCAYMEM	AE	MCAYGM	AE	MCAYEM	AE
June	14.48	13.74	0.74	14.87	0.46	13.94	0.54
July	101.14	101.56	0.42	101.04	0.10	100.83	0.31
August	49.95	49.15	0.80	49.73	0.22	49.69	0.26
September	69.97	69.76	0.21	69.25	0.72	70.22	0.25

and the second part is modeling of the magnitude or amount of rainfall on a wet day. In the first part, a Markov chain with analogue year component (MCAY) model is used in order to model the frequency of the rainfall occurrence. In the second component of the model that is amount or magnitude modeling part, we consider three different distributions namely exponential distribution, gamma distribution and mixed exponential distribution. The result of the study reveals all the three models performs very well. Both qualitative (graphical) and quantitative techniques are used in order to assess their performance. Quantitatively the performance of the three models; MCAYEM, MCAYGM and MCAYMEM are measured using mean absolute error (MAE). All the three models have nearly the same performance in all the three stations. The mean absolute errors in monthly cumulative rainfall are 0.45mm, 0.57mm and 0.42mm respectively for kiremet (June to September) rainfall which is the long rainy season in all parts of Ethiopia. Based on the result of the developed rainfall models we calculated an option price for Teff crop using monthly cumulative rainfall. The pricing results are quite

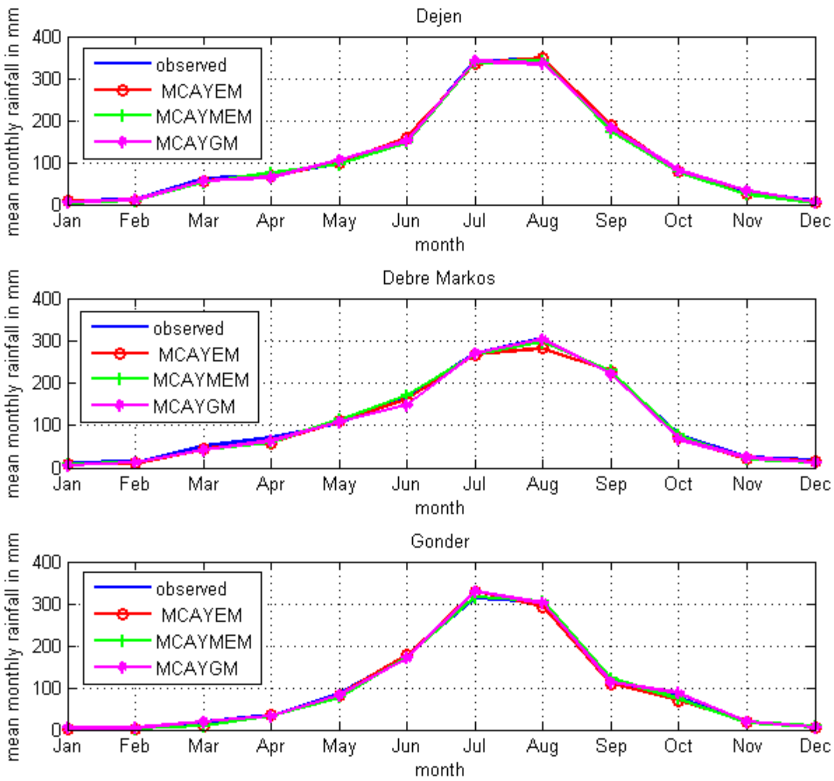

Figure 14. Average montly rainfall using (a) MCAYMEM, (b) MCAYMEM, (c) MCAYMEM (top to bottom) respectively and observed monthly average rainfall of Dejen, Debre Markos and Gonder from 1987 to 2015.

accurate in all models with only maximum absolute error of 0.34 currency in MCAYEM, 0.36 currency in MCAYGM and 0.54 currency in using MCAYMEM. Therefore the main contribution of the paper is incorporating Analogue Year (AY) component in the Markov chain (MC) in the modeling of frequency of daily rainfall which improves the accuracy of the model in an excellent way.

References

[1] H. Aksoy, Use of gamma distribution in hydrological analysis, Turkish Journal of Engineering and Environmental Sciences, **24 (6)** (2000) 419–428.

[2] P. Alaton, B. Djehiche and D. Stillberger, On modelling and pricing weather derivatives, Applied mathematical finance, **9 (1)** (2002) 1–20.

[3] R. G. Allen, L. S. Pereira, D. Raes and M. Smith, Crop evapotranspiration-guidelines for computing crop water requirements-fao irrigation and drainage paper 56, Fao, Rome, (1998).

[4] W. Bewket, Rainfall variability and crop production in ethiopia: Case study in the amhara region, in: Proceedings of the 16th International Conference of Ethiopian Studies, Vol. 3, Norwegian University of Science and Technology Trondheim, Norway, (2009) 823–836.

[5] C. Bhavana, R. Munirajappa, H. Surendra and S. RATHOD, Modeling of daily rainfall using gamma probability distribution, Environment and Ecology, **30 (3B)** (2012) 884–887.

[6] N. Bird, Fair share: climate finance to vulnerable countries, London: Overseas Development Institute, (2014).

[7] P. J. Block, F. A. Souza Filho, L. Sun and H.-H. Kwon, A streamflow forecasting framework using multiple climate and hydrological models 1, JAWRA Journal of the American Water Resources Association, **45 (4)** (2009) 828–843.

[8] B. L. Cabrera, M. Odening and M. Ritter, Pricing rainfall derivatives at the CME, Humboldt University, Berlin, Germany, (2013).

[9] L. Cochrane and Y. W. Bekele, Average crop yield (2001–2017) in ethiopia: Trends at national, regional and zonal levels, Data in brief, **16** (2018) 1025–1033.
[10] M. Cao, A. Li and J. Z. Wei, Precipitation modeling and contract valuation: A frontier in weather derivatives, The Journal of Alternative Investments, **7 (2)** (2004) 93–99.
[11] S. Di Falco, M. Yesuf, G. Kohlin and C. Ringler, Estimating the impact of climate change on agriculture in low-income countries: household level evidence from the nile basin, ethiopia, Environmental and Resource Economics, **52 (4)** (2012) 457–478.
[12] J. Doorenbos, A. Kassam and C. I. M. Bentvelsen, Yield response to water, FAO irrigation and drainage paper, Food and Agriculture Organization of the United Nations (1979).
[13] F. Hagos, G. Makombe, R. Namara and S. B. Awulachew, Importance of irrigated agriculture to the ethiopian economy: capturing the direct net benefits of irrigation, IWMI Research Reports 61100, International Water Management Institute, (2009).
[14] J. Geyser, Weather derivatives: concept and application for their use in south africa, Agrekon, **43 (4)** (2004) 444–464.
[15] M. Gezie, Farmers response to climate change and variability in ethiopia: A review, Cogent Food & Agriculture, **5 (1)** (2019) 1613770.
[16] A. Goncu, Modeling and pricing precipitation-based weather derivatives, Financial Mathematics and Applications, **1 (1)** (2011) 9–18.
[17] P. Y. Groisman, T. R. Karl, D. R. Easterling et al., Changes in the probability of heavy precipitation: important indicators of climatic change, Climatic Change, **42** (1999) 243–283.
[18] D. Guida, A. Longobardi and P. Villani, Hydrological modelling for river basin management in a highly hydro-geological conditioned environment, WIT Transactions on Ecology and the Environment, **89** (2006) 283-292.
[19] L. S. Hanson and R. Vogel, The probability distribution of daily rainfall in the united states, in: World Environmental and Water Resources Congress, (2008) 1–10.
[20] M. Holden, Chloroplast pigments in plants with the c4-dicarboxylic acid pathway of photosynthesis, Photosynthetica, (1973).
[21] G. J. Husak, J. Michaelsen and C. Funk, Use of the gamma distribution to represent monthly rainfall in africa for drought monitoring applications, International journal of Climatology, **27 (7)** (2007) 935–944.
[22] A. V. Ines and J. W. Hansen, Bias correction of daily gcm rainfall for crop simulation studies, Agricultural and forest meteorology, **138 (1-4)** (2006) 44–53.
[23] S. Kang, B. Gu, T. Du and J. Zhang, Crop coefficient and ratio of transpiration to evapotranspiration of winter wheat and maize in a semi-humid region, Agricultural water management, **59 (3)** (2003) 239–254.
[24] S. K. Kannan and J. A. Farook, Stochastic simulation of precipitation using markov chain-mixed exponential model, Applied Mathematical Sciences, **65 (9)** (2015) 3205–3212.
[25] R. W. Katz, Extreme value theory for precipitation: sensitivity analysis for climate change, Advances in Water Resources, **23 (2)** (1999) 133–139.
[26] H. Kebede, R. Johnson and D. Ferris, Photosynthetic response of eragrostis tef to temperature, Physiologia Plantarum, **77 (2)** (1989) 262–266.
[27] H. Lee, Teff, a rising global crop: Current status of teff production and value chain, The Open Agriculture Journal, **12 (1)** (2018) 185–193.
[28] G. Leobacher and P. Ngare, On modelling and pricing rainfall derivatives with seasonality, Applied Mathematical Finance, **18 (1)** (2011) 71–91.
[29] A. Leon-Garcia, Probability, Statistics, and Random Processes for Electrical Engineering, Pearson/Prentice Hall, (2008).
[30] G. Makombe, D. Kelemework and D. Aredo, A comparative analysis of rainfed and irrigated agricultural production in ethiopia, Irrigation and Drainage Systems, **21 (1)** (2007) 35–44.
[31] S. W. Martin, B. J. Barnett and K. H. Coble, Developing and pricing precipitation insurance, Journal of Agricultural and Resource Economics, 26 (1) (2001) 261-274.
[32] O. Musshoff, M. Odening and W. Xu et al., Modeling and pricing rain risk, in: 26th Conference of the International Association of Agricultural Economists, Gold Coast, Australia, (2006).
[33] M. Odening, O. Mußhoff and W. Xu, Analysis of rainfall derivatives using daily precipitation models: Opportunities and pitfalls, Agricultural Finance Review, **67 (1)** (2007) 135–156.
[34] M. Osman and P. Sauerborn, A preliminary assessment of characteristics and long term variability of rainfall in ethiopia–basis for sustainable land use and resource management, Conference on Agricultural Research for Development, Deutscher Tropentag Witzenhausen, (2002).
[35] C. Piani, J. Haerter and E. Coppola, Statistical bias correction for daily precipitation in regional climate models over europe, Theoretical and Applied Climatology, **99 (1-2)** (2010) 187–192.
[36] J. Piantadosi, J. Boland and P. Howlett, Generating synthetic rainfall on various timescalesdaily, monthly and yearly, Environmental Modeling & Assessment, **14 (4)** (2009) 431–438.
[37] C. W. Richardson, Stochastic simulation of daily precipitation, temperature, and solar radiation, Water resources research, **17 (1)** (1981) 182–190.
[38] M. Ritter, O. Musshoff and M. Odening, Minimizing geographical basis risk of weather derivatives using a multi-site rainfall model, Computational Economics, **44 (1)** (2014) 67–86.
[39] K. Rosenberg, J. Boland and P. Howlett, Simulation of monthly rainfall totals, ANZIAM Journal, **46** (2004) 85–104.
[40] A. Seifu, Rainfall variation and its effect on crop production in ethiopia, Masters diss. Addis Ababa University, School of Graduate Studies.
[41] A. Shenkut, K. Tesfaye and F. Abegaz, Determination of water requirement and crop coefficient for sorghum (sorghum bicolor l.) at melkassa, ethiopia, Science, Technology and Arts Research Journal, **2 (3)** (2013) 16–24.
[42] P. Steduto, T. C. Hsiao, E. Fereres and D. Raes, et al., Crop yield response to water, Vol. 1028, fao Rome, 2012.

[43] R. Stern and R. Coe, A model fitting analysis of daily rainfall data, Journal of the Royal Statistical Society: Series A (General), **147 (1)** (1984) 1–18.
[44] M. Stowasser, Modelling rain risk: a multi-order markov chain model approach, The Journal of Risk Finance, **13 (1)** (2011) 45–60.
[45] J. Suhaila and A. A. Jemain, Fitting the statistical distribution for daily rainfall in peninsular malaysia based on aic criterion, Journal of Applied Sciences Research, **4 (12)** (2008) 1846–1857.
[46] A. Tefera and G. Quintin, Ethiopia: grain and feed annual report, Global Agricultural Information Network, USDA Foreign Agriculture Service, Report Number ET 1201, (2012).
[47] P. Todorovic and D. A. Woolhiser, A stochastic model of n-day precipitation, Journal of Applied Meteorology, **14 (1)** (1975) 17–24.
[48] D. V. Vedenov and M. J. Miranda, Rainfall insurance for midwest crop production, 2001 Annual meeting, Chicago, IL 20458, American Agricultural Economics Association, (2001).
[49] R. Wilby, B. Greenfield and C. Glenny, A coupled synoptic-hydrological model for climate change impact assessment, Journal of Hydrology, **153 (1-4)** (1994) 265–290.
[50] D. S. Wilks, Maximum likelihood estimation for the gamma distribution using data containing zeros, Journal of Climate, **3 (12)** (1990) 1495–1501.
[51] D. S. Wilks, Statistical Methods in the Atmospheric Sciences, Academic press, (2011).
[52] D. S. Wilks and R. L. Wilby, The weather generation game: a review of stochastic weather models, Progress in physical geography, **23 (3)** (1999) 329–357.
[53] D. A. Woolhiser, et al., Stochastic daily precipitation models: 1. a comparison of occurrence processes, Water resources research, **18 (5)** (1982) 1451–1459.
[54] D. A. Woolhiser and G. Pegram, Maximum likelihood estimation of fourier coefficients to describe seasonal variations of parameters in stochastic daily precipitation models, Journal of Applied Meteorology, **18 (1)** (1979) 34–42.
[55] M. Yenesew and K. Tilahun, Yield and water use efficiency of deficit-irrigated maize in a semi-arid region of ethiopia, African Journal of Food, Agriculture, Nutrition and Development, **9 (8)** (2009) 1635-1651.
[56] L. Zeng, Pricing weather derivatives, The Journal of Risk Finance, **1 (3)** (2000) 72–78.
[57] O. Zolina, C. Simmer, A. Kapala, S. Bachner, S. Gulev and H. Maechel, Seasonally dependent changes of precipitation extremes over germany since 1950 from a very dense observational network, Journal of Geophysical Research: Atmospheres, **113 (D6)** (2008), doi: 10.1029/2007JD00839.